JOURNAL OF SOLID STATE CHEMISTRY 84, 58–70 (1990)

Temperature-Resolved X-Ray Powder Diffractometry of a New Cadmium Hydroxide Nitrate

J. P. AUFFREDIC, J. PLEVERT, AND D. LOUËR

Laboratoire de Cristallochimie (UA 254), Université de Rennes, Avenue du Général Leclerc, F-35042 Rennes Cedex, France

Received May 8, 1989; in revised form July 24, 1989

A new cadmium hydroxide nitrate, $Cd_3(OH)_5NO_3$, was prepared by an interdiffusion method and its X-ray powder diffraction pattern was indexed. The symmetry is orthorhombic and the cell parameters are $a = 3.4209(3)$ Å, $b = 10.0292(6)$ Å, and $c = 11.0295(6)$ Å. The thermal decomposition of this solid was analyzed in a vacuum and in a nitrogen atmosphere by the TG, MS, and TRXD methods. Temperature-resolved diffractometry was carried out by means of a curved position-sensitive detector combined to a conventional X-ray powder diffractometer. A new modification of $Cd(OH)NO_3$ was displayed during the first stage of the decomposition and a detailed decomposition scheme is proposed. This study shows that the rate of the structural transformation can be quite different from that of the departure of the gaseous molecules. From TRXD, the evolution of microstructural properties of $Cd(OH)NO_3$ and CdO as a function of temperature is also described.

Introduction

Among the recent developments of the powder diffraction technique, the time-resolved diffractometry appears to be a useful tool for the investigation of structural changes occurring in materials. Applications have been greatly improved by the advent of high-power radiation sources and new position-sensitive detectors (PSD) combined to efficient data storage. Examples based on the use of synchrotron radiation and neutron sources have been described (see, for example, Refs. (*1–3*)). Applications have also been done with conventional X-ray diffractometers, combined to standard or to position-sensitive detectors in some laboratories for characterizing microstructural (*4*) and structural (see, for example, Refs. (*5, 6*)) modifications due to solid state transformations. In a recent paper, we also described the kinetics of a phase transformation occurring in the dicesium cadmium tetraoidide at room temperature (*7*). The present paper deals with the temperature-resolved diffractometry of a new cadmium hydroxide nitrate studied by means of a conventional diffractometry system combined with a curved position-sensitive detector. The benefits of this kind of approach in current chemical studies of phase changes as well as the complementary features of this technique with the usual thermal methods are discussed.

Two well defined cadmium hydroxide nitrates have already been described: $Cd(OH)NO_3 \cdot H_2O$ (*8*), whose layer crystal structure is related to β-$Cd(OH)_2$ type, and $Cd(OH)NO_3$ (*9*), which is characterized by a tridimensional structure. Moreover, from

0022-4596/90 $3.00

a general point of view, cadmium hydroxide and related hydroxide salts frequently present several different forms. Three modifications of the hydroxide are known and the crystal structure of four cadmium hydroxide sulfates have been described (*10*). Consequently, it was interesting to consider the possibility of synthesis of new cadmium nitrate hydroxides. Although the preparation of basic salts with soft conditions by means of an interdiffusion method has already been described (*11*), it seems that this technique has not been applied frequently. In the present paper the synthesis of a new cadmium hydroxide nitrate characterized by a low content in substituant nitrate anion and the indexing of its powder diffraction pattern are described. The thermal behavior of this solid is also studied by means of the temperature-resolved X-ray diffractometry (TRXD) and the usual thermal analysis methods. Moreover, the evolution with the temperature of microstructural (crystallite sizes and microstrains) properties of the solids involved in the transformation is also discussed.

Experimental Considerations

The TG analysis was carried out using a Rigaku Thermoflex TG-DSC. About 10 mg of the powdered sample was well thoroughly spread on a large platinum sample holder in order to avoid mass effect and to reproduce as much as possible the conditions used in the temperature-resolved diffractometry study.

To determine the sequence of the removal of the gaseous molecules from the solids during their decomposition in a high vacuum, a mass spectrometer (MS) VARIANT MAT 311 was used.

For the precise characterization of the powder compound by diffraction and for accurate line-broadening analysis a Siemens D500 powder diffraction system was employed. Strictly monochromatic $CuK\alpha_1$ radiation (1.5405981 Å) was produced with an incident-beam curved-crystal germanium monochromator with asymmetric focusing (short focal distance = 124 mm, long focal distance = 216 mm). The powder diffraction data were collected by step scanning (step = 0.02°(2θ)). The adjustment of the diffractometer was checked by using standard materials. The accuracy at low angles was evaluated by means of the 001 reflections of a fluorophlogopite mica material available from NBS (SRM 675).

For the time-resolved diffractometry the X-ray data acquisition was performed by means of a INEL (CPS120) cylindrical position-sensitive detector, which allows for a simultaneous recording of a powder pattern over a range of 120°. The detector was used in a semifocusing arrangement by reflection. Strictly monochromatic $CuK\alpha_1$ radiation (λ = 1.5405981 Å) was selected by means of an incident-beam curved-crystal quartz monochromator with asymmetric focusing (short focal distance = 130 mm, long focal distance = 510 mm). The stationary powder sample is located at the center of the goniometer (R = 250 mm) and intercepts the convergent x-ray beam, which is focused on the goniometer circle. The curved PSD coincides with the goniometer circle. A fixed angle θ_i of 6° between the incident beam and the surface of the sample was selected. This means that parafocusing is only obtained for a diffracted beam located at 12°(2θ). This arrangement combined with an incident beam limited by a slit of 0.2 wide, located at a distance of 70 mm before the sample, to restrict the diffracting area of the sample, ensures satisfactory diffraction line profiles over a useful angular range. The data acquisition was performed by the PSD with a spatial resolution of about 0.03°(2θ). The time interval between successive powder patterns was 1150 sec, including a measuring time of 1000 sec. The data were stored in a PDP 11-73 computer.

The integrated intensities of some lines for the different phases were evaluated by fitting Pearson VII functions to raw experimental data. An example of fitting for the 220 line of the powder diffraction pattern of cadmium oxide registered at 330°C is shown in Fig. 1. The 3D plot of the collected data was performed by means of a computer program locally written for a HP-7475A plotter.

The sample was located in a high-temperature X-ray diffractometer attachment (Rigaku) designed to maintain a specimen at high temperature either in a vacuum, inert gas or in the ambient atmosphere. The furnace was combined with a program temperature controller. To avoid mass effect during the decomposition the powder was deposited in a thin layer on a nickel grid used as a sample holder.

Synthesis and Powder Pattern Indexing

The new cadmium hydroxide nitrate was prepared at room temperature by means of an interdiffusion method in aqueous media, as described by de Haan (*11*). By means of a pipette, a 2 *M* solution of cadmium nitrate was carefully introduced at the bottom of a glass container previously three-fourths filled with distilled water. The container was connected to a similar one filled with 2 *M* ammonia. After a few hours, the new compound was formed. The microcrystalline solid, characterized by a fibrous texture, was mixed with some crystals having a hexagonal platelet shape, identified as β-$Cd(OH)_2$. For subsequent analysis, these hexagonal crystals must be eliminated. The formula $Cd_3(OH)_5NO_3$ was found from the chemical analysis of the cadmium and TG measurements. The Cd content, 69.75 ± 0.40%, was found to be in accordance with the expected value (69.42%). From the thermal decomposition of this compound, the weight loss for the decomposition into CdO was 20.40% (theoretical value: 20.45%).

For the indexing of the powder pattern of

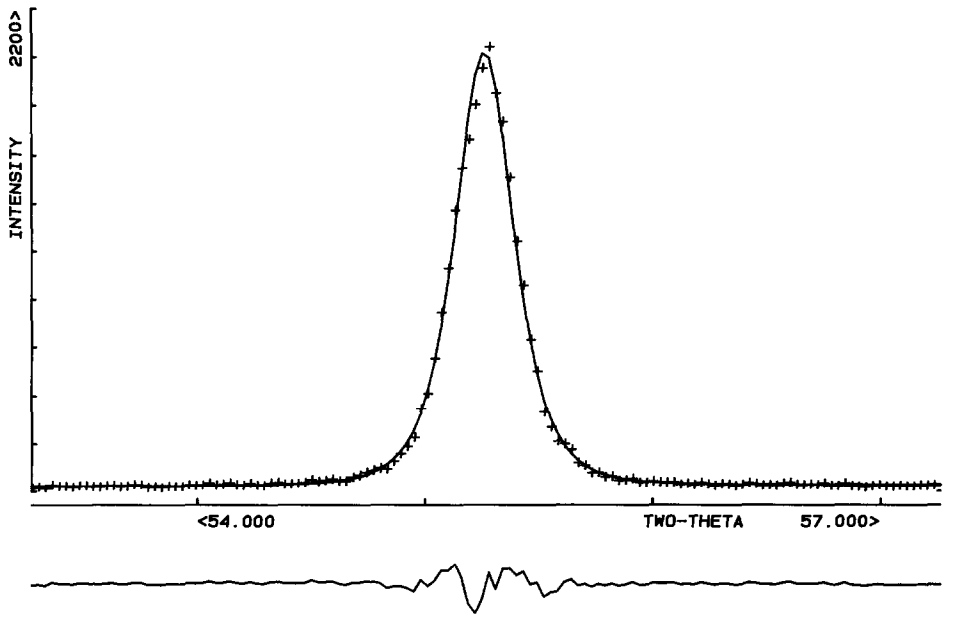

FIG. 1. Example of individual peak fit and difference plot for the 220 reflection of CdO obtained from the PSD (Pearson VII model, m index = 2.15, R_{wp} = 7.8%).

the new compound, a careful evaluation of the peak positions was carried out by means of the fitting program FIT (*12*) available in the Siemens software system. The first 20 lines of the pattern were used as input data in the indexing program DICVOL (*13, 14*), which is based on the variation of direct parameters by means of a dichotomy procedure. An absolute error bound of 0.03°(2θ) for each diffraction line was used. Only one solution was obtained; the symmetry is orthorhombic with the unit cell parameters:

a = 3.4206(4) Å, b = 10.0269(12) Å,
c = 11.0282(11) Å, V = 378.25 Å^3.

The reliability of the unit cell and indexing is indicated by the figures of merit (*15, 16*) M_{20} = 117 and F_{20} = 157(0.0043, 30). The quality of the data can also be evaluated by the average absolute magnitude of the discrepancy between observed and calculated 2θ values, i.e., $\Delta 2\theta$ = 0.0043°. The proposed unit cell indexes all the observed lines of the diffraction pattern (Table I). It can be noted that the first eight consecutive lines are $0kl$ reflections; in spite of that, this example demonstrates that the successive dichotomy method is insensitive to one common zero index for all the first lines of the pattern. After a least-squares refinement from the complete list of observed

TABLE I

X-RAY POWDER DIFFRACTION DATA OF $Cd_3(OH)_5NO_3$

h	k	l	$2\theta_{obs}$ (°)	$2\theta_{cal}$ (°)	d_{obs} (Å)	I	h	k	l	$2\theta_{obs}$ (°)	$2\theta_{cal}$ (°)	d_{obs} (Å)	I
0	0	1	8.025	8.010	11.01	80	0	2	5	44.854	44.856	2.0191	5
0	1	1	11.925	11.917	7.42	100	1	4	1	45.58	45.568	1.9886	6
0	0	2	16.070	16.059	5.511	1<	0	5	1	45.96	45.949	1.9731	3
0	1	2	18.340	18.345	4.834	1<	1	2	4		49.950		
0	2	1	19.432	19.430	4.564	87	1	1	5	49.995	49.994	1.8229	5
0	2	2	23.970	23.966	3.710	2	1	3	4	50.49	50.484	1.8061	17
0	0	3	24.190	24.191	3.676	1<	1	4	3	51.530	51.536	1.7721	3
0	1	3	25.794	25.791	3.451	18	0	5	3	51.886	51.885	1.7608	4
1	0	1	27.286	27.273	3.266	7	1	2	5	52.584	52.593	1.7390	4
1	1	0	27.53	27.527	3.237	1	0	2	6	53.009	53.018	1.7261	1<
0	3	1	27.869	27.864	3.199	6	2	0	0	53.56	53.533	1.7096	11
1	1	1	28.716	28.713	3.106	34	1	5	1		53.567		
0	2	3	30.119	30.118	2.965	21	2	0	1	54.24	54.226	1.6898	1<
1	0	2	30.733	30.732	2.907	23	0	6	0	54.883	54.882	1.6715	6
0	3	2	31.265	31.263	2.859	38	2	1	1	55.049	55.055	1.6669	4
0	0	4	32.447	32.447	2.757	45	0	4	5	55.45	55.437	1.6558	2
1	2	1	32.68	32.686	2.738	17	0	6	1	55.56	55.563	1.6527	2
0	1	4	33.686	33.686	2.659	4	1	5	2	55.63	55.625	1.6508	1
0	4	1	36.745	36.729	2.4439	7	1	3	5	56.743	56.737	1.6211	7
1	1	3	36.967	36.968	2.4297	10	1	0	6	56.81	56.816	1.6193	7
1	3	0	37.589	37.589	2.3909	41	2	2	0		56.827		
1	3	1	38.502	38.496	2.3363	6	0	3	6	57.15	57.141	1.6105	8
0	4	2	39.44	39.448	2.2829	1<	2	2	1	57.49	57.494	1.6018	3
1	2	3	40.212	40.219	2.2408	8	0	6	2	57.60	57.572	1.5590	4
0	0	5	40.880	40.881	2.2057	5	1	1	6		57.620		
0	1	5	41.902	41.903	2.1543	9	1	5	3	58.91	58.947	1.5665	3
0	3	4	42.466	42.462	2.1270	1<	0	1	7	59.33	59.329	1.5564	1
0	4	3	43.660	43.662	2.0715	3							

lines the parameters were

$a = 3.4209(3)$ Å, $b = 10.0292(6)$ Å, $c = 11.0295(6)$ Å.

From the list of the unambiguous peaks detected in the powder pattern, it was seen that all lines could be indexed using the restriction $hk0$, $h + k = 2n$, in agreement with the presence of a glide plane n parallel to (001). The quality of the powder pattern allowed for the determination of the *ab initio* crystal structure of this material from the powder data with the space group *Pmmn* (*17*).

Thermal Properties of Cadmium Hydroxide Nitrate: Environmental Effects

1. Thermal Decomposition in Nitrogen

Thermal analysis by TRXD and TG. The thermal decomposition of the cadmium nitrate hydroxide was carried out at a heating rate of 5 K hr^{-1}. A three-dimensional representation of the evolution of the powder diffraction patterns with temperature is shown on Fig. 2. With the increase of temperature, the powder diffraction diagrams correspond successively to a mixture of an unknown phase and cadmium oxide, to a mixture of cadmium nitrate and cadmium oxide, and finally to pure cadmium oxide. The integrated intensities of the diffraction lines (011) for $Cd_3(OH)_5NO_3$, (111) for $Cd(NO_3)_2$, (220) for CdO, and the line located at 13.35°(2θ) for the new compound are presented as a function of the temperature in Fig. 3; the TG curve obtained under the same experimental conditions is also shown. For $Cd_3(OH)_5NO_3$, the choice of the (011) line, located at 11.925°(2θ), close to the line at 13.35°(2θ), allowed for a simultaneous fit of the two lines. It can be seen that the decomposition of $Cd_3(OH)_5NO_3$ starts at about 160°C and in the first stage this solid transforms into the new unknown solid and CdO simultaneously up to 210°C. At this temperature the TG curve presents a very slight inflection point for a value of $\Delta m/m_0$ close to 8%, while the amount of the new phase reaches a maximum and the rate of CdO formation passes through a minimum. The second stage of the decomposition takes place at a narrow temperature range (210–230°C) where the unknown compound simultaneously gives CdO and the cubic modification of $Cd(NO_3)_2$ (*18*). Its total disappearance corresponds approxi-

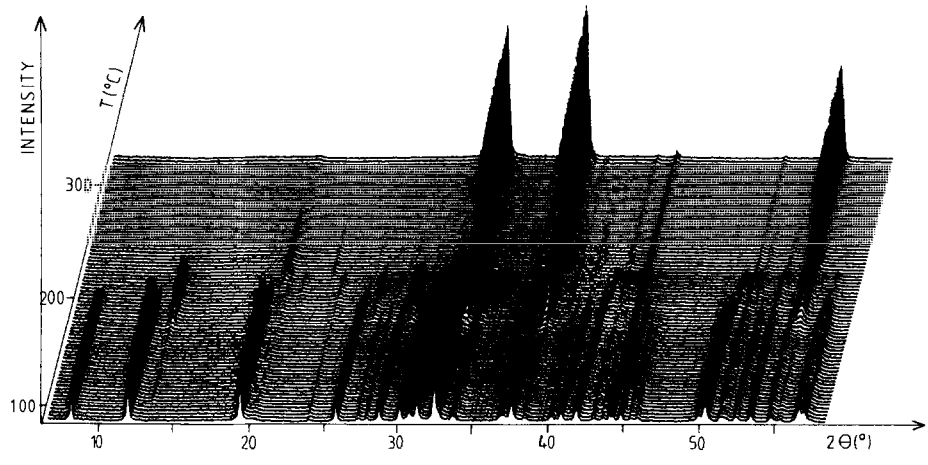

FIG. 2. The TRXD plot of $Cd_3(OH)_5NO_3$ in nitrogen gas (heating rate, 5 K hr^{-1}; counting time for each pattern, 1000 sec).

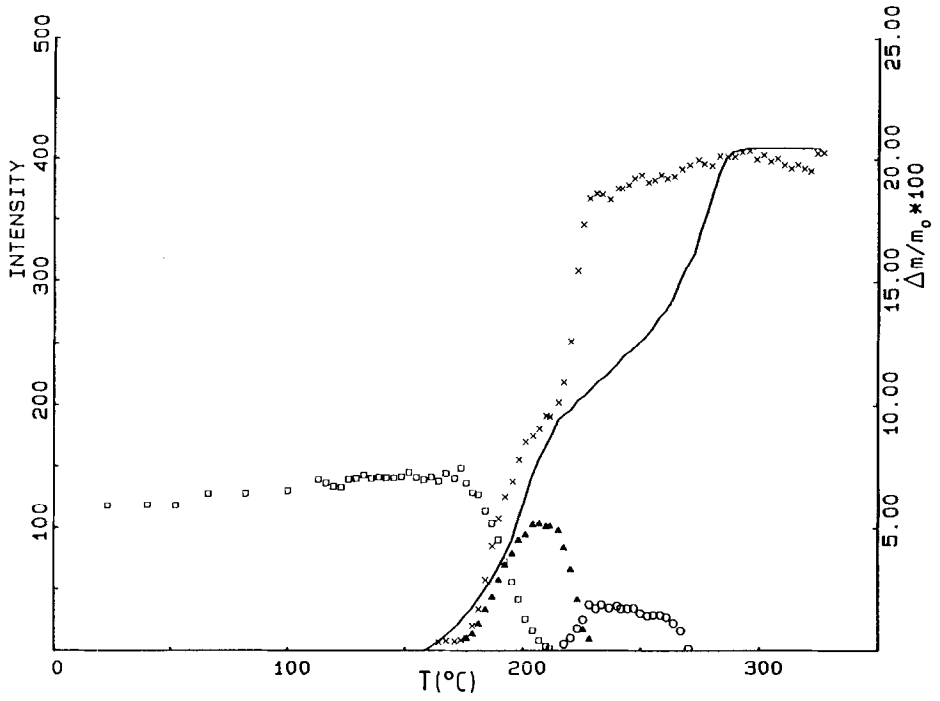

FIG. 3. Integrated intensities of *hkl* diffraction lines vs temperature from the TRXD in nitrogen. (□) 001 $Cd_3(OH)_5NO_3$, (×) 220 CdO, (▲) first line of the unknown phase, (○) 111 cubic $Cd(NO_3)_2$. The full line represents the TG curve.

mately to the second inflection point which is observed on the TG curve for $\Delta m/m_0$ close to 10%. The last step is characterized by the decomposition of $Cd(NO_3)_2$ into CdO.

In an effort to determine the chemical formula of the unknown phase, several TG runs were performed at selected constant temperatures between 160 and 210°C. The precursor was heated with a heating rate of 100 K hr^{-1} from the room temperature up to the selected temperature, and then maintained at this latter temperature for many hours and finally cooled to room temperature. The solid obtained was identified from X-ray powder diffraction analysis. From this study it can be concluded that:

—First, the mass loss for which the powder diffraction pattern corresponds only to the mixture of the unknown phase and CdO is approximately $\Delta m/m_0 = 7.3\%$. It is obtained at 178°C after about 30 hr. This mass loss corresponds well to the departure of two water molecules from the precursor. Consequently, this experiment proves that $Cd_3(OH)_5NO_3$ transforms into $Cd(OH)NO_3$ and CdO according to the reaction

$$Cd_3(OH)_5NO_{3(cr)} \rightarrow Cd(OH)NO_{3(cr)} + 2CdO_{(cr)} + 2H_2O_{(g)}. \quad (1)$$

—Second, above 180°C, the $Cd(OH)NO_3$ phase transforms slowly into a second Cd $(OH)NO_3$ modification, whose crystal structure has been previously described (*9*). This transformation is clearly displayed on the 3D plot shown in Fig. 4, obtained from 175 to 195°C by successive temperature jumps of 5°C over a period of 24 hr. The modification obtained at low tempera-

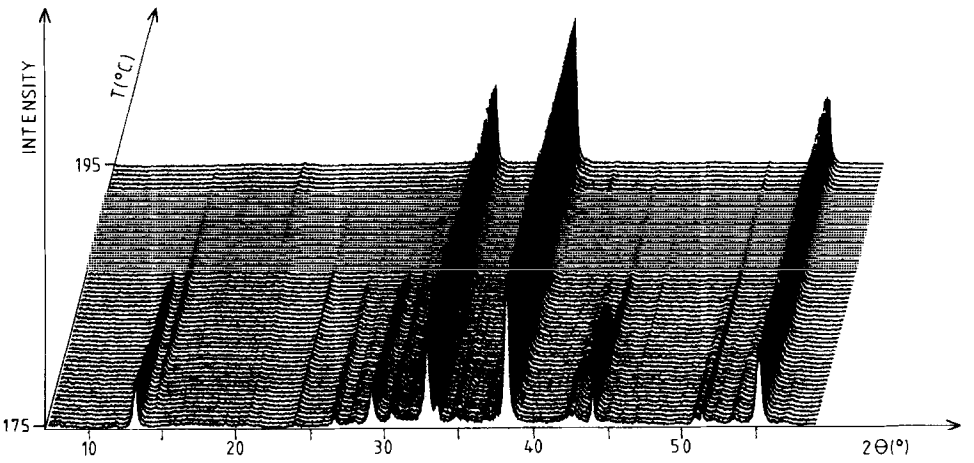

FIG. 4. The TRXD plot of the transformation α-$Cd(OH)NO_3 \rightarrow \beta$-$Cd(OH)NO_3$.

ture is α-$Cd(OH)NO_3$, while the second modification is β-$Cd(OH)NO_3$. This α phase is also obtained in the first stage of the decomposition of the hydroxysalt $Cd(OH)NO_3 \cdot H_2O$, as verified in the course of this study. An interesting feature of these two anhydrous phases concerns their rehydration into $Cd(OH)NO_3 \cdot H_2O$ at room temperature and ambient atmosphere. The rehydration of the α phase seems dependent on its precursor. When it is obtained from $Cd(OH)NO_3 \cdot H_2O$, it rehydrates rapidly, while it is stable when it is obtained from $Cd_3(OH)_5NO_3$. On the contrary, the β phase rehydrates whatever its precursor. The powder diffraction pattern of β-$Cd(OH)NO_3$ is in agreement with the data published by Nguyen *et al.* (*19*), with the exception of the first line of the latter (located at $13.36°2\theta$), which has been identified as the strongest line of the powder pattern of the α phase. The powder diffraction data of the new α-$Cd(OH)NO_3$ are given in Table II. The accuracy of these data is low due to significant line broadening and indexing attempts were unsuccessful.

From this study, the successive steps of the decomposition of $Cd_3(OH)_5NO_3$ can be written

$$Cd_3(OH)_5NO_{3(cr)} \rightarrow \alpha\text{-}Cd(OH)NO_{3(cr)} + 2\ CdO_{(cr)} + 2\ H_2O_{(g)} \quad (2)$$

$$\alpha\text{-}Cd(OH)NO_{3(cr)} \rightarrow \beta\text{-}Cd(OH)NO_{3(cr)} \quad (3)$$

$$\alpha\text{- or } \beta\text{-}Cd(OH)NO_{3(cr)} \rightarrow \tfrac{1}{2}\ Cd(NO_3)_{2(cr)} + \tfrac{1}{2}\ CdO_{(cr)} + \tfrac{1}{2}\ H_2O_{(g)} \quad (4)$$

$$\tfrac{1}{2}\ Cd(NO_3)_{2(cr)} \rightarrow \tfrac{1}{2}\ CdO_{(cr)} + m/2\ NO_{(g)} + (2 - m)/2\ NO_{2(g)} + (1 + m)/4\ O_{2(g)}, \quad (5)$$

where $0 \leq m \leq 2$. The calculated weight loss for the reactions (2), (4), and (5) are 7.43, 9.29, and 20.44%, respectively. This latter value is in excellent accordance with the observed value (20.40%). The fact that the first two values do not exactly correspond to the inflection points on the TG curve (Fig. 3) indicates that the reactions (2) and (4) on the one hand and (4) and (5) on the other superimpose. Moreover, it can be noted that, due to the very low rate of the transformation (3), the decomposition of the α phase according to the reaction (4) is observed before its transformation into

TABLE II

X-RAY POWDER DIFFRACTION DATA OF α-$Cd(OH)NO_3$

$2\theta_{obs}$ (°)	d_{obs} (Å)	I
13.350	6.63	100
20.050	4.43	3
21.670	4.10	5
24.200	3.67	7
24.350	3.65	5
26.930	3.31	20
28.180	3.16	7
29.250	3.05	65
29.410	3.03	45
30.620	2.92	11
30.770	2.90	17
33.710	2.66	40
35.230	2.55	13
37.760	2.38	13
42.570	2.122	18
51.070	1.787	10
52.090	1.754	10
53.660	1.707	8
56.900	1.617	7
59.270	1.558	4
60.590	1.527	6
64.010	1.453	4

the β phase when the experiments are carried out in a nonisothermal mode even if the heating rate is as low as 5 K hr^{-1}. This feature of the transformation $\alpha \rightarrow \beta$ also appears during the cooling, since the β phase does not transform into the α phase.

Microstructural properties of α-$Cd(OH)NO_3$, CdO, and $Cd(NO_3)_2$. Due to the limited amount of available data on one specific powder pattern, and as a consequence of the medium resolution owing to the defocusing effect of the diffraction geometry used and to the great number of lines to be interpreted, an approximate single-line Voigt analysis (*20*) was used. A discussion on the accuracy of such a practice will be presented later. In this Voigt procedure it is assumed that the Cauchy component of the structurally broadened profile is solely due to crystallite size and that the Gaussian contribution arises from microstrains. This treatment gives an estimation of the volume-weighted crystallite size D and a microstrain parameter e averaged over all the coherence lengths perpendicular to the diffracting planes. In the present study the e values are less than 5×10^{-4}, which can be considered as negligible compared to the crystallite size effect. The crystallite sizes D as a function of T (°C) during the decomposition process are given in Table III. These sizes were obtained from the line located at 13.35°(2θ) of the pattern of α-$Cd(OH)NO_3$, the 220 line for CdO and the 111 line for $Cd(NO_3)_2$. It is noted that the α-$Cd(OH)NO_3$ and CdO appearing in the primary stage of the decomposition phase have very small crystallites and that a fast crystallite growth occurs between 200 and 230°C.

2. *Thermal Decomposition in a Vacuum*

Thermal analysis by TRXD and TG. The three-dimensional representation of the temperature evolution of the powder diffraction patterns of the cadmium hydroxide nitrate is shown in Fig. 5. Compared to Fig. 2, some differences can be seen. If, as described above, the formation of α-$Cd(OH)NO_3$ and CdO is simultaneous, on

TABLE III

CHANGES IN CRYSTALLITE SIZES D (Å) AS A FUNCTION OF TEMPERATURE FROM A VOIGT ANALYSIS OF SOME DIFFRACTION LINES

T (°C)	α-$Cd(OH)NO_3$ (line at 13.35°(2θ))	CdO (220)	$Cd(NO_3)_2$ (111)
192	430	320	
198	890	420	
204	1340	600	
215	1500	840	
220	∞[a]	1600	
225	∞	∞	
233			580
240			640
245			650

[a] ∞ denotes $D > 1600$ Å.

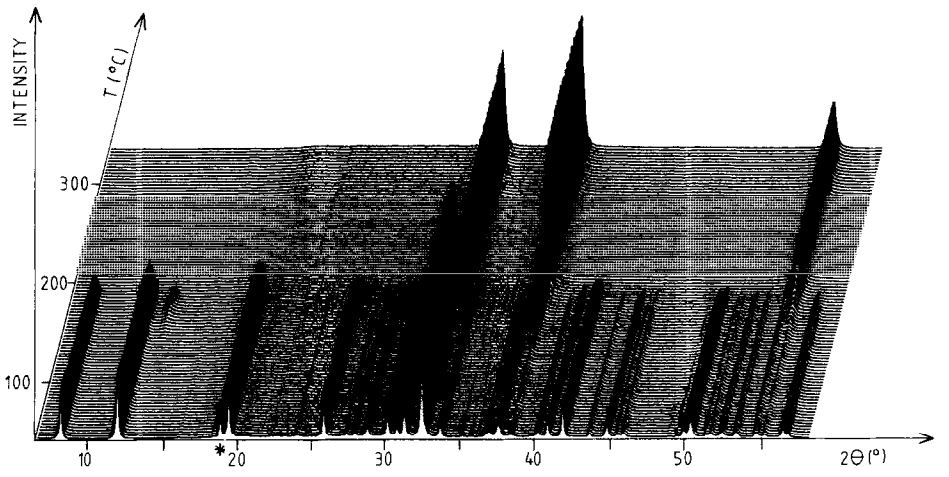

FIG. 5. The TXRD plot of $Cd_3(OH)_5NO_3$ in a vacuum (heating rate, 5 K hr^{-1}; counting time for each pattern, 1000 sec). * Spurious diffraction line of 001 reflection of β-$Cd(OH)_2$.

the other hand the cadmium nitrate is not detected during the thermal decomposition. Another feature is the weakness and the extreme broadening of the diffraction lines of α-$Cd(OH)NO_3$. The integrated intensities were found by fitting Pearson VII functions to four lines. In order to evaluate the precision of the measures two lines with different orders, the well resolved and strong line 001 and the strong line 004 appearing in a cluster of lines, were selected for the precursor. The results can be seen in Fig. 6. The decomposition seems to occur in only one step, as shown by the variation of integrated intensities vs temperature for some diffraction lines of CdO, α-$Cd(OH)NO_3$, and $Cd_3(OH)_5NO_3$. In the temperature range 200 to 300°C no subsequent increase of the line intensity for CdO is observed. On the contrary, the TG curve shows that the weight loss is not complete up to 300°C. Moreover, it presents an inflection point at about 200°C for $\Delta m/m = 9.5\%$.

To explain this apparent discordance between TG and TRXD analyses, the precursor was heated at a heating rate of 5 K hr^{-1} under a vacuum of 1.33×10^{-2} Pa up to 230°C where $\Delta m/m_0 = 15.80\%$, then rapidly cooled to room temperature, and finally kept under dynamic vacuum for 16 hr. The obtained product was pure CdO as revealed by XRD, which corroborates with the results obtained by TRXD. Moreover, a MS analysis of the gaseous molecules arising from the thermal decomposition was carried out in a high vacuum of 1.33×10^{-5} Pa at a heating rate of 600 K hr^{-1} (Fig. 7). This analysis indicates that the decomposition of the nitrate groups begins to take place at 180°C, at the same time as the departure of H_2O molecules, and becomes more important at a temperature greater than 300°C, where the total amount of hydroxyl groups have disappeared. It can be assumed that these features are also similar when the heating rate is lower, which is the case for the TG and TRXD analyses. These complementary experiments are consistent with a much lower rate of the departure of NO, NO_2, and O_2 from the solid than the rate of the structural transformation. This situation has already been described by many authors (*21, 22*). It would seem that the gases, more particularly NO, NO_2, and O_2, remain adsorbed on the finely divided solids produced and that their desorption is

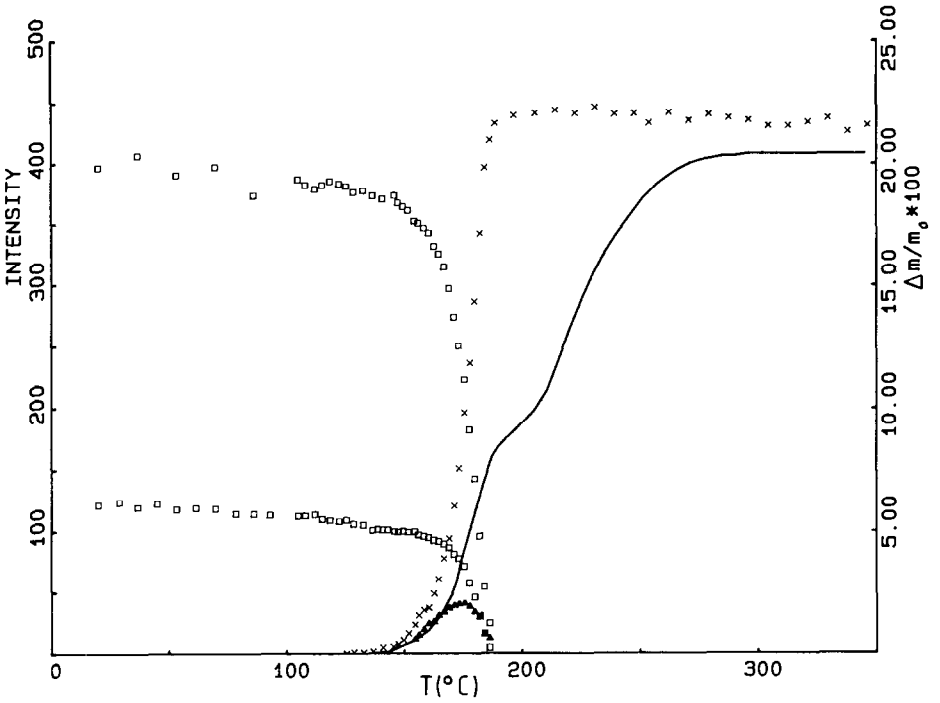

FIG. 6. Integrated intensities of *hkl* diffraction vs temperature from the TRXD in a vacuum. (□) 001, 004 $Cd_3(OH)_5NO_3$, (×) 200 CdO, (▲) first line of the α-$Cd(OH)NO_3$. The full line represents the TG curve.

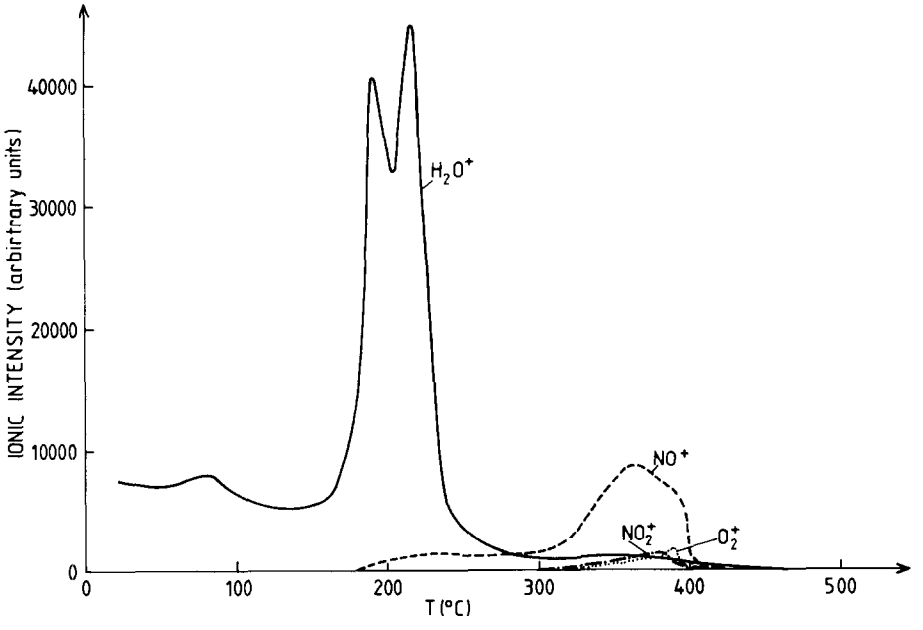

FIG. 7. Ionic intensities of H_2O^+, NO^+, NO_2^+, and O_2^+ vs temperature during the decomposition of $Cd_3(OH)_5NO_3$ in a vacuum (heating rate, 600 K hr^{-1}).

difficult. This effect is more pronounced in the experiment carried out in vacuum; it can be noted that the crystallite size of cadmium oxide (about 210 Å) is significantly smaller in this case compared to the size of diffracting domains obtained under atmospheric pressure (Table III). According to the TRXD analysis, the thermal decomposition of $Cd_3(OH)_5NO_3$ in vacuum would take place in two strongly superimposed stages corresponding to the following reactions,

$$Cd_3(OH)_5NO_{3(cr)} \rightarrow \alpha\text{-}Cd(OH)NO_{3(cr)} + 2CdO_{(cr)} + 2H_2O_{(g)} \quad (2)$$

$$\alpha\text{-}Cd(OH)NO_{3(cr)} \rightarrow CdO_{(cr)} + m/2\ NO_{(g)} + (2 - m)/2\ NO_{2(g)} + (1 + m)/4\ O_{2(g)} + \tfrac{1}{2}\ H_2O_{(g)}, \quad (6)$$

without formation of cadmium nitrate.

Microstructural analysis of CdO. The single-line Voigt analysis was used to obtain an estimation of the size of the coherently diffracting domains of CdO. As indicated above, this method is approximate and gives only an estimation of the crystallite sizes. In the temperature range 200–350°C the crystallite size increases slowly from 450 to 650 Å. Compared to the experiment in nitrogen the crystallite growth in a vacuum is observed at higher temperature.

In order to have a correspondence with the true absolute size, a Fourier analysis of the 200/400 and 220/440 diffraction lines was carried out on a CdO sample obtained at 300°C by decomposition of $Cd_3(OH)_5NO_3$ in vacuum. The diffraction lines were registered by step-scanning, using the Bragg-Brentano focusing geometry with strictly monochromatic radiation. The treatment was carried out by means of an on-line computer program locally written. The correction for instrumental broadening was performed by the Stokes deconvolution method by using an annealed CdO sample as standard material. The Fourier coefficients A_L vs L for the 200/400 diffraction lines are shown in Fig. 8. From this figure it is seen that the Fourier transforms superimpose quite well, bearing in mind the low intensity of the 400 reflection. This is an indication of negligible microstrains in the material. A similar superposition of Fourier transforms was observed for the 220/440 diffraction lines. From the initial slope of the Fourier transforms, after correction of the small hook effect, surface-weighted crystallite sizes in directions perpendicular to the (h00) and (hh0) planes were obtained. They are, namely, 144 and 116 Å respectively. To compare these to the values obtained from the simple Voigt method previously used, it is necessary to determine the volume-weighted apparent crystallite size obtained from the integral breadth, which can be deduced from the reciprocal of ΣA_L. These sizes are respectively 232 and 188 Å in directions perpendicular to h00 and hh0 planes. The ratio between the size obtained by the approximate single line method and the rigorous Fourier analysis is about 2.5. Moreover, it is interesting to note that the cadmium oxide which is obtained is strain-free. Indeed, the synthesis of strain-free materials is not so frequent; such a situation usually depends on the chemical parameters used during the reaction. An extensive study on zinc oxide obtained from the decomposition of a zinc hydroxynitrate has already been described (*23*). The fact that the microstrains are negligible has allowed for the demonstration that a precise analysis of the diffraction line broadening could give accurate information about the morphological characters of the crystallites. In the case of cadmium oxide resulting from the decomposition of the cadmium hydroxide nitrate studied in this paper, it can also be mentioned that anisotropic morphology of the diffracting domains exists, owing to the sig-

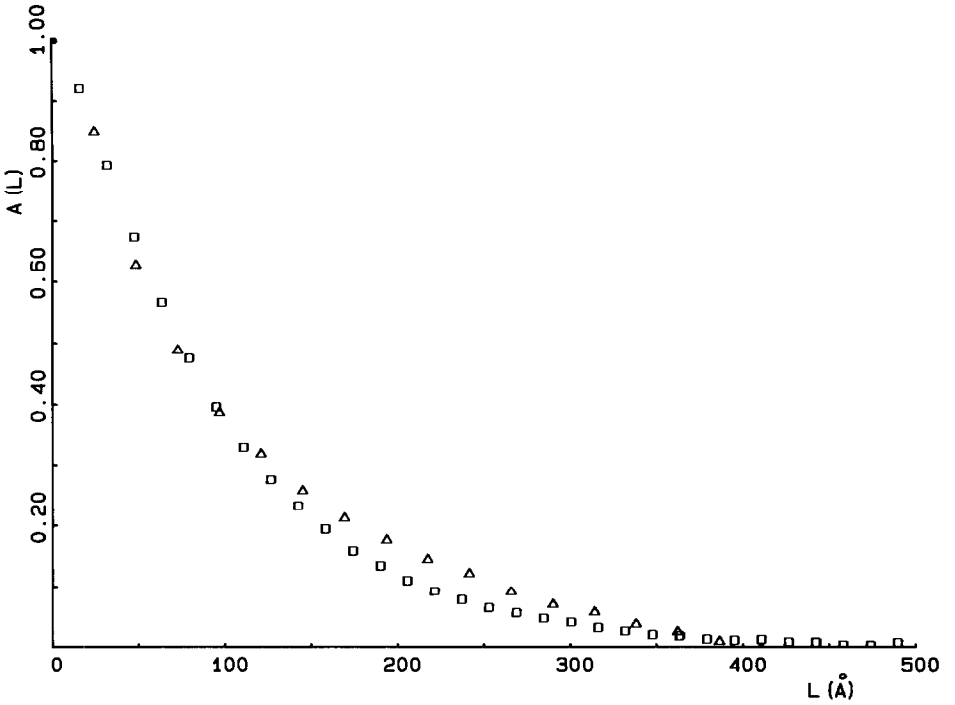

FIG. 8. Fourier cosine coefficients A_L vs L for CdO. (□) 200 diffraction line, (△) 400 diffraction line.

nificant size differences in two directions of the reciprocal space (100 and 110). The interpretation of this observation is however more complicated than that in the case of zinc oxide, owing to the effect of the multiplicity of *hkl* planes for a cubic symmetry (*24*).

Conclusion

The TRXD technique resulting from the coupling of conventional X-ray powder diffractometry and a position-sensitive detector appears as a powerful tool for thermostructural analyses of materials. With the use of a curve detector useful structural and microstructural (crystallite sizes and strains) parameters can be traced as a function of the temperature in a single experiment. Although some defocusing effects arise from the diffraction geometry described above, the results which have been obtained demonstrate the power of this technique for the study of the thermal decomposition of solids. Consequently, it appears as a necessary complement to the other thermal analysis methods such as TG, DSC, and MS, which are commonly used in the analysis of the structural changes occurring in solids.

In this study, a new cadmium hydroxide nitrate $Cd_3(OH)_5NO_3$, characterized by a low nitrate content, was prepared by means of an interdiffusion method and its thermal behavior was analyzed. The different stages which occur during decomposition were clearly displayed by the TRXD technique. From this study two modifications of $Cd(OH)NO_3$ were identified. Moreover, the role of environment on the successive stages of the decomposition was evidenced by the experiments in a vacuum and in a nitrogen atmosphere; it was shown that the structural transformation and the departure

of the gaseous molecules evolving from the solids may not be simultaneous, as is demonstrated in the last stage of the decomposition of $Cd_3(OH)_5NO_3$ when the experiment is carried out in a vacuum. Finally, valuable information from the broadening of the diffraction lines about the estimation of crystallite sizes and microstrains was obtained for $Cd(OH)NO_3$, $Cd(NO_3)_2$, and CdO as a function of temperature. Furthermore, strain-free cadmium oxide was obtained when the decomposition reaction was carried in a vacuum.

Acknowledgments

The authors thank Mr. C. Hervieu and Mr. G. Marsolier for their technical assistance.

References

1. Ö. Sävborg, J. R. Schoonover, S. H. Lin, and L. Eyring, *J. Solid State Chem.* **68,** 214 (1987).
2. J. R. Schoonover and S. H. Lin, *J. Solid State Chem.* **79,** 143 (1988).
3. J. Pannetier, *Chem. Scr. A* **26,** 131 (1986).
4. A. Le Bail and D. Louër, *Rev. Chim. Minér.* **17,** 522 (1980).
5. T. G. Fawcett, E. J. Martin, C. E. Crowder, P. J. Kincaid, A. J. Strandjord, J. A. Blazy, D. N. Armentrout, and R. A. Newmann, *Adv. X-ray Anal.* **27,** 323 (1986).
6. P. Engler, N. W. Santana, M. L. Mittleman, and D. Balazs, *Thermochim. Acta* **130,** 309 (1988).
7. J. Plevert, J. P. Auffredic, M. Louër, and D. Louër, *J. Mater. Sci.* **24,** 1913 (1989).
8. A. M. T. Nievelstein, Y. M. de Haan, and W. J. A. M. Peterse, *Acta Crystallogr. Sect. A* **25,** S117 (1969).
9. A. M. Rodriguez Roldan, M. Louër, J. P. Auffredic, and D. Louër, *Acta Crystallogr. Sect. C* **39,** 418 (1983).
10. D. Louër, J. Labarre, J. P. Auffredic, and M. Louër, *Acta Crystallogr. Sect. B* **38,** 1079 (1982).
11. Y. M. de Haan, *Nature (London)* **200,** 876 (1963).
12. D. W. Marquardt, *J. Soc. Ind. Appl. Math* **11,** 431 (1963).
13. D. Louër and M. Louër, *J. Appl. Crystallogr.* **5,** 271 (1972).
14. D. Louër and R. Vargas, *J. Appl. Crystallogr.* **15,** 542 (1982).
15. P. M. de Wolff, *J. Appl. Crystallogr.* **1,** 108 (1968).
16. G. S. Smith and R. L. Snyder, *J. Appl. Crystallogr.* **12,** 60 (1979).
17. J. Plevert, M. Louër, and D. Louër, *J. Appl. Crystallogr.* (1989), **22,** in press.
18. M. Louër, D. Louër, and D. Grandjean, *J. Solid State Chem.* **17,** 231 (1976).
19. D. Nguyen, D. Louër, and D. Weigel, *C.R. Acad. Sci. Paris* **269,** 1444 (1969).
20. Th. H. de Keijser, J. I. Langford, E. J. Mittemeijer, and A. B. P. Vogels, *J. Appl. Crystallogr.* **15,** 308 (1982).
21. W. Sthählin and H. R. Oswald, *J. Solid State Chem.* **3,** 252 (1971).
22. J. P. Auffredic and D. Louër, *J. Solid State Chem.* **46,** 245 (1983).
23. J. P. Auffredic and D. Louër, *React. Solids* **4,** 105 (1987).
24. J. C. Niepce, M. Th. Mesnier, and D. Louër, *J. Solid State Chem.* **22,** 341 (1977).